GKSS
FORSCHUNGSZENTRUM
in der HELMHOLTZ-GEMEINSCHAFT

Final Draft
of the original manuscript:

Scheu, C.; Sterger, E.; Schober, M.; Cha, L.; Clemens, H.; Bartels, A.;
Schimansky, F.-P.; Cerezo, A.:

High Carbon Solubility in a gamma-TiAl based Ti-45Al-5Nb-0.5C Alloy and its Effect on Hardening

In: Acta Materialia (2009) Elsevier

DOI: 10.1016/j.actamat.2008.11.037

* Text only

High Carbon Solubility in a γ-TiAl based Ti-45Al-5Nb-0.5C Alloy and its Effect on Hardening

C. Scheu [a,b,*], E. Stergar [a], M. Schober [a], L. Cha [a], H. Clemens [a], A. Bartels [c], F.-P. Schimansky [d] and A. Cerezo [e]

[a] *Department of Physical Metallurgy and Materials Testing, University of Leoben, Roseggerstr. 12, A-8700 Leoben, Austria*

[b] *Department of Chemistry and Biochemistry, Ludwig-Maximilians-University of Munich, Butenandtstr. 5-13 (E), 81377 Munich, Germany*

[c] *Materials Science and Technology,Technical University Hamburg Harburg, Eißendorfer Str. 42, D-21073 Hamburg, Germany*

[d] *Institute of Materials Research, GKSS Research Center, Max Planck Str. 1, D-21502 Geesthacht, Germany*

[e] *Department of Materials, Oxford University, Parks Road, Oxford OX1 3PH, United Kingdom*

**Corresponding author/Present address:*
Christina Scheu, Phone: 0049-89-2180-77184, Fax: 0049-89-2180-77622,
e-mail: Christina.Scheu@cup.uni-muenchen.de

Abstract

The C distribution within the γ-TiAl-phase of a Ti-45Al-5Nb-0.5C alloy with near-γ microstructure has been studied by atom probe tomography. In most areas the C atoms are homogenously distributed, and only a few C enriched features were detected which are presumably Cottrell atmospheres surrounding dislocation cores. The C concentration within the γ-phase was measured to be approximately 0.25 at.%, which is a factor of ten higher than the solubility limit reported for other TiAl alloys. The reason for this unusually high C solubility is explained by an existing model which relates the number of octahedral sites consisting of six Ti atoms to the solubility limit of interstitials. The large amount of C in solid-solution can explain the results of a recent study which showed that the C-containing alloy had an approximately 30% increase in yield strength when compared with a C-free sheet containing the same Ti, Al and Nb concentration.

Keywords: three-dimensional atom probe (3DAP), titanium aluminides, carbon, interstitials, mechanical properties

1. Introduction

Due to their outstanding properties, such as low weight, high strength, good creep performance and high oxidation-resistance, γ-TiAl based titanium aluminides are promising high-temperature materials and are already in use for automotive and aircraft applications [1-3]. Binary two-phase γ-TiAl based alloys possess good high-temperature properties, but they often suffer from low room temperature ductility [4-6]. This can be overcome by alloying with elements such as Nb, Mo, V, Mn and Cr [6, 7]. Recent developments have shown that alloys containing 5-10 at% Nb exhibit high room-temperature ductility together with high creep and oxidation resistance [8-10].

Interstitial elements such as C, O and N, which might be present as impurities or alloy additions, also modify strongly the room temperature ductility either by degrading or by improving the strength [6, 11]. In the particular case of C the effect is beneficial due to both solid-solution hardening and formation of C-containing precipitates [12]. These are either cubic Ti_3AlC Perovskite-phase ("P"-phase) or hexagonal Ti_2AlC-phase ("H"-phase) precipitates which form depending on thermal treatment and aging conditions [12, 13]. Typical age-hardening behaviour is observed where the strength is increasing with the formation of precipitates [12, 14, 15]. It was shown that dislocations are effectively pinned by these precipitates [12, 16, 17]. In contrast, it was reported that C in solid-solution is a weak obstacle for dislocation gliding which can be easily overcome by thermal activation [16, 17]. These studies were restricted to binary TiAl alloys, and did not address whether other alloying elements such as Nb might modify the solid-solution strengthening behaviour of C.

Recently, we reported that the mechanical properties of Ti-45Al-5Nb (all compositions are in atomic %) sheets with near-γ microstructure are significantly improved by the addition of 0.5 at.% C, although the microstructure remained very similar [18]. For example, the room temperature (RT) tensile yield strength increased from around 800 MPa for the C-free case to 1070 MPa for the C-containing sheet [18]. We speculated that the improved performance of the C-containing sheet is mainly due to a solid-solution hardening effect of C, since the techniques we used to investigate the microstructure of the sheets, i.e.

transmission electron microscopy (TEM), X-ray diffraction (XRD), and small-angle neutron scattering (SANS), did not gave any evidence for the presence of C-containing precipitates [18]. The aim of the present work is to confirm that C is indeed contained in solid-solution within the γ-phase at a level that can account for the hardening effect. For this purpose, we used atom probe tomography (APT) [19] which allows determination of the local chemical composition within the γ-phase, and visualisation of the atomic-scale distribution of the carbon atoms.

Back in 1986, Menand and co-workers performed first atom probe investigations on TiAl alloys [20] and since then this technique has been successfully applied to study near-γ TiAl alloys [21-23], lamellar (α_2-Ti_3Al + γ-TiAl) two-phase alloys [22-33] and duplex microstructures [34, 35]. Most of this research was dedicated to identifying the partitioning behaviour of alloying elements and impurities within the different phases. Comprehensive and thorough investigations of the distribution of C and O within various TiAl alloys were made by Menand and co-workers [21, 22, 24]. They found that C and O preferentially locate in the α_2-phase. The measured C and O levels within the γ-phase were extremely low, at 0.02-0.03 at.% (200-300 appm). These values remained constant for different binary alloys as well as for various ternary alloys which all contained C and O as impurities with levels of around 0.05 at.% and 0.25 at.%, respectively. The ternary alloys included Nb-doped material with nominal compositions of Ti-52Al-3Nb and Ti-51Al-5Nb. From their studies Menand and co-workers concluded that the maximum solid-solubility limit of C and O in the γ-phase is 200-300 appm, independent of the alloy composition. Indeed, measurements by Kim et al. in γ-lamellae of a Ti-48Al-2Cr alloy, which contained impurity levels of 0.15-0.2 at.% O and 500-600 appm C, revealed similar low C and O concentrations [26]. However, Qin et al. [28] found a higher O content in the γ-phase of a Ti-47Al-2Nb-1Cr-1V alloy which ranged between 600-800 appm, depending on the heat treatment. The C concentration within γ-lamellae was again lower than 300 appm. Gerstl et al. studied a multi-component TiAl alloy (Ti-46.5Al-1.5Cr-0.5Mn-3Nb-0.2W-0.2Hf-0.2Zr-0.2B-0.2C-0.2O), and found that both the C and O concentration in were much higher in

the γ-phase than the values reported by Menand and co-workers, and amounted to 1500 appm and 800 appm for C and O, respectively [35]. Gerstl et al. speculated that this might be related to the multi-component nature of the investigated alloy though no possible explanation for this was given.

In the present work, we have made use of two different atom probe instruments, which have enabled us to obtain atomic-scale C distributions from far larger sample volumes than was previously possible, but also to determine the chemical composition of smaller volumes with high precision. We have investigated a Ti-Al-Nb engineering alloy containing carbon, of a composition not previously studied by atom probe tomography.

2. Material and Experimental Details

Investigated Material

The material was prepared via a powder-metallurgical based process. Starting from an alloy powder with a composition Ti-45Al-5Nb-0.5C, compacts were made by hot-isostatic pressing for 2h at 1270°C and 200MPa [18]. The compacts were then multi-passed rolled within the (α + γ) phase field. Subsequently, the obtained sheets with dimensions of 600x440x1.2 mm^3 were primary annealed at 1050°C for 2h. More details about the production and treatment of the sheets are given elsewhere [18]. The C content was measured by a conventional melt extraction system (CS-444 system, LECO, USA) and amounted to the nominal value of 0.5 at.% [18].

The general microstructure of the sheet after primary annealing is shown in the scanning electron micrograph (SEM) displayed in Fig. 1a. In this back-scattered electron image the γ-grains appear grey to black, and the α_2-grains appear white. The microstructure consists of equiaxed γ-grains with an average size of about 6µm, which are embedded in a mixture of smaller, 1-3µm sized α_2- and γ-grains [18]. A large number of annealing and mechanical twins are visible within the larger γ-grains. Fig. 1b shows as an example a TEM micrograph of such twins. In addition, the γ-grains contain dislocations. A few are marked in Fig. 1b. The volume fraction of the γ- and α_2-phase was determined XRD, SEM and light microscopy and amounted to 80 vol. % and 20 vol. %, respectively [18].

Atom probe tomography

For APT measurements the rolled and primary annealed sheets were cut into bars with dimensions of 0.35x0.35x15 mm^3, with the long axis of the bars parallel to the rolling direction. From these bars, needle-shaped specimens were prepared using a standard two-stage procedure [19]. The initial polishing step was performed with a 25% perchloric acid in acetic acid at 25-30 V dc, while for the second stage a solution consisting of 2% perchloric acid in 2-butoxyethanol and a dc voltage of 15-20V was used. Some of the samples were back-polished using a micro-loop setup applying the same parameters as for second-stage polishing. All polishing was performed at room temperature.

Atom probe analyses were conducted on a 3-dimensional energy-compensated atom probe (3DAP^{TM}-LAR from Oxford Nanoscience, UK) at the University of Leoben, Austria, and on a local-electrode atom probe (LEAP^{TM}3000XSi from Imago, USA) at the University of Oxford, UK. The LEAP is equipped with a picosecond pulsed laser system and was operated in laser mode using a pulse rate of 250 kHz and a pulse energy of 1 nJ. Under laser pulsing, the mass-resolution was limited by the time spread of the evaporating ions, resulting from the time taken for the specimen to cool down after the laser pulse. Individual mass-to-charge ratio peaks showed an asymmetrical shape, with extended tails toward the higher atomic mass-to-charge side. Consequently, the LEAP data were mainly used to analyse qualitatively the C distribution over large sample volumes. High precision chemical compositions of the γ-grains were obtained from voltage-pulsed measurements in the energy-compensated 3DAP, where a higher mass resolution was obtained. For these measurements, the pulse to standing voltage was kept constant at 15%, as proposed in literature to prevent preferential evaporation [19].

All atom probe measurements were conducted at a temperature of 70K - 80K to avoid fracture of the material. More than ten investigations containing up to 55 million atoms were performed. Only those datasets containing more than 2 million atoms were considered for further analysis.

3. Results

Reconstructed atom maps of Ti, Al, Nb and C atoms from 3DAP analysis of the γ-phase of the investigated Ti-45-Al-5Nb-0.5C alloy are displayed in Fig. 2. All atoms are homogenously distributed within the analysed volume. In particular, there is no indication that C-containing precipitates are formed. The analysed volume has a length of about 250 nm and a cross-section increasing from approximately 30x30 nm^2 to 60x60 nm^2 during the measurement. It contains around 11 million atoms. The γ-phase mass spectra of the 3DAP measurements revealed that Ti and Al are mainly detected as doubly-charged ions ($^{48}Ti^{+2}$ and $^{27}Al^{+2}$), in agreement with the literature [21, 22, 26]. Nb was detected either as triply-charged $^{93}Nb^{+3}$ ions or as doubly-charged $^{93}Nb^{+2}$ ions. For C the main peak corresponded to $^{12}C^{+}$, however, a minor peak related to $^{12}C^{+2}$ ions was observed. Again, this is in agreement with published data [21, 22, 26]. Nb and C are also detected as molecular $(NbC)^{+2}$ ions. It is worth mentioning that this does not mean that NbC precipitates are present in the material, which otherwise would have been detected by our TEM and SANS measurements too. Furthermore, a cluster algorithm [36] did not give any evidence of clusters containing Nb or C larger than 10 atoms (equivalent to a size of 20 atoms in the material). Thus, the $(NbC)^{+2}$ ions form during the APT analyses, as a result of Nb and C atoms close together on the surface evaporating as a molecular ion rather than as individual atomic species.

In addition to Ti, Al, Nb and C, the mass spectra indicated the presence of some Si impurities which are detected as $^{28}Si^{+2}$ and $^{28}Si^{+}$ ions (see also Fig. 2). A small peak was found at a mass-to-charge-ratio of 32 amu (atomic mass unit) which can correspond to molecular $(TiO)^{+2}$ ions or O_2^{+}. A further peak was detected at 16amu which can be attributed to $^{48}Ti^{+3}$ or to $^{16}O^{+}$. Menand and co-workers developed a method to separate these signals by using standard values for isotope abundance ratios of the $^{48}Ti^{+3}$ peaks [21, 22]. As in the study of Kim et al. [26], the peak at 16 amu corresponded in our case to Ti^{+3} ions. Furthermore, since no $(TiO)^{+2}$ isotope abundance peaks were detected, we concluded that O is mainly in the state of O_2^{+} (corresponding to the peak at 32 amu).

The chemical composition of the analysis volume shown in Fig. 2 is summarized in Table 1. The small error bar of each concentration value is related to the high counting statistics. The Ti content is 49.81 ± 0.03 at.%, the Al content amounts to 44.21 ± 0.02 at.%, and the Nb concentration is 5.54 ± 0.01 at.%. Atom probe analysis of different γ-grains resulted in average values of 49.1 ± 0.7 at.% for the Ti content, 45.1 ± 0.9 at.% for the Al concentration and 5.4 ± 0.2 at.% for the Nb content (the error bar is the maximum absolute error). It is worth mentioning that similar values were measured by energy-dispersive X-ray spectroscopy in the TEM. A significant underestimation of the Al content as reported by Wesemann et al. [29] was not found in the present study. The observed variation of the grain composition is typical for large sheets produced with industrial standard. Similar or even larger variations in the chemical composition were observed for other Ti-Al alloys [14, 29]. Concerning the minor elements, all of our data show similar levels of C (2580 ± 30 appm), Si (1440 ± 240 appm) and very low levels of O (130 ± 30 appm). The numbers present average values for the concentrations and the corresponding maximum error obtained by using measurements of different γ-grains. The result for a measurement within one γ-grain is given in Table 1. The averaged concentrations are listed in Table 2.

Using laser pulsing in the LEAP, we were able to analyse large volumes within a relatively short acquisition time. Fig. 3a shows three-dimensional Ti, Al, Nb, C and Si maps from part of the analysed volume. For the C map $^{12}C^{+}$, $^{12}C^{+2}$ ions as well as $^{12}C^{+2}$ ions from molecular $(NbC)^{+2}$ ions were taken into consideration. The reconstruction represents a volume of around 60x60x750 nm^3 and contains about 55 million atoms. The overall chemical composition of this γ-grain was estimated to amount to Ti ≈ 50 at.%, Al ≈ 44 at.%, Nb ≈ 4,2 at.% at., C ≈ 1150 appm, Si ≈ 600 appm and O ≈ 40 appm. While the values for the main elements Ti and Al are in agreement with the 3DAP measurements, Nb, C, Si and O are underestimated. As mentioned above, the differences are most likely due to the long tails of the mass peaks, which are observed in laser pulsing, affecting the quantification. Nevertheless, we can use the data to get further confirmation of

the C distribution within the γ-phase on a larger scale. As for the 3DAP data, in most areas the C is homogenously distributed. However, two apparently parallel C-enriched rod-like structures occur in the reconstruction volume. These features extend from one surface to the other and possess a length of around 80 nm and a width of 2-4 nm. An enlarged view of the topmost of these carbon-rich features is given in Fig. 3b. Composition analyses of these features were made by using cylinders with diameters of around 5 nm. Within these cylinders the C level was >1.2 at.%, the Ti concentration was increased to ≈ 60 at.%, while the Al content decreased to ≈ 34 at.%. The Nb, Si and O concentration were similar to that in the bulk.

It is worth mentioning that we detected a similar amount of homogenously distributed Si atoms in the C-free sheet (unpublished data) as in the C-containing sheet. Therefore, in the following discussion we neglect the effect of Si since it is assumed to be similar in both materials and thus needs not to be considered when comparing the strength of the two sheets.

4. Discussion

Distribution of C in the γ-phase of Ti-45Al-5Nb-0.5C

Atom probe investigations of the γ-phase of a Ti-45Al-5Nb-0.5C alloy have confirmed that C is indeed contained in solid-solution, in agreement with our recently published TEM, XRD and SANS results [18]. None of the applied techniques give any indication for the formation of C-containing precipitates as a result of the applied heat treatment. This is in agreement with the results of Chen et al. who also detected no precipitates in Ti-48Al-2Nb-0.2C alloys after a heat treatment of 1100°C for 1-2 hours followed by water-quenching [13]. However, in contrast to the TEM methods employed by Chen and co-workers our atom probe investigations allow us unambiguously to rule out the presence of nanometer-sized precipitates.

It is worth mentioning that the size of the analysis volume obtained in the APT studies presented here is much larger than that of previously published atom probe studies of TiAl alloys, e.g. [21, 22, 24]. The number of detected atoms is

a factor of 100 higher and this allows us not only to obtain data with high statistical confidence but also to analyze the distribution of C on a larger scale. The results show that C is homogenously distributed in most areas of the γ-phase. Only two C enriched features were detected. These are most probably dislocations where C is preferentially segregated. The distance between the observed two features is around 500 nm, consistent with the separation between dislocations visible in Fig. 1b. The detection of such Cottrell atmospheres by APT had already been reported previously in other alloys [37-40]. The observed widths and enrichments of segregated elements in the different cases were always of the same order, amounting to 2-6 nm and a factor of 5 to 20 compared to the bulk, respectively, similar to the present work. For example, Blavette et al. [37] showed the presence of B-enriched Cottrell atmospheres around edge-dislocations in a B2-ordered FeNi alloy. They observed a boron enrichment of 2 at.%, which was 50 times higher than in the bulk, and a depletion of Al by 20 at.%. The width of the Cottrell atmosphere was in the range of 3 – 5 nm [37].

An additional advantage of accessing large reconstruction volumes is that the data can be directly compared to TEM investigations. Earlier TEM studies [12, 13, 16, 17] have revealed typical C-containing precipitates of 20 -100 nm in length and 3-6 nm in width, which form arrays with a spacing of about 50-100nm. If a similar distribution was present in our material, we would have detected several precipitates within our analysed APT volume as well as observing them in the TEM, e.g. in electron diffraction patterns, which was not the case. However, it is tempting to speculate that the observed C Cottrell atmospheres are preferential sites for precipitate formation which might occur at longer aging treatments. It is unlikely that the C-enriched features measured by APT are already precipitates since (i) the amount of C within the features is too low for precipitates, (ii) they extend from one surface to the other which is typical for dislocations, and (iii) no additional reflections have been found in electron diffraction patterns.

Comparison of C Solubility in Ti-45Al-5Nb-0.5C to Literature Values

As mentioned previously, most atom probe analyses revealed a similar low C and O concentration of ≈ 300 appm in the γ-phase, as found by Menand and co-workers [21, 22, 24], and these values had been accepted to present upper limits for the C and O solubility in the γ-phase. Only the results of the present work and of the studies of Gerstl et al. [35] and Qin et al. [28] seem not to agree with these literature values, indicating much higher C and/or O concentrations.

To shed light on what might be responsible for these differences, a comparison of the chemical composition of the γ-phase in various Nb- and/or Cr/V-bearing TiAl alloys containing C and O is given in Table 2. All data were measured by atom probe analysis and were taken from [22, 26, 28, 35] and from the present work. It is obvious that the amount of C and O, which is present in the γ-phase, depends for the investigated Nb- and/or Cr/V-containing alloys on the Ti/Al ratio. If the Ti concentration is lower than the Al concentration or close to the stoichiometric value of 1:1, the C and O levels are similar and lower than 400 appm. For the cases, where the Al concentration is lower (≈ 45 at.%) than the Ti concentration (≈ 50 at.%), the O and/or the C concentration are increasing by factors between 2 and 25. Note, that only in the work of Gerstl et al. [35] and in the present study C and/or O was intentionally added to the alloys with a relatively high amount, in the other studies they were present as impurities. However, for the alloys investigated by [22, 26, 28] the O impurity level was high and amounted to 0.1 – 0.25 at.% while the C impurity content was around 250-600 appm. Thus, these alloys can also be considered to have considerable C and O levels but they show a low C and O concentration within the γ-phase.

It is tempting to speculate about possible reasons for this behaviour. For this it is important to describe in detail the empirical model derived by Menand and co-workers [22, 24] with which they explained the low solubility limits of C and O in the γ-phase of binary TiAl alloys. The main idea of the model is that interstitials prefer octahedral sites consisting of six Ti atoms ("Ti_6-type"), which exist in the DO_{19} structure of the α_2-phase, and this explains its high C and O solubility [22, 24]. In contrast, the octahedral sites of the $L1_0$ structure of the γ-phase always possess a surrounding of mixed atom type, consisting either of four Al and two

Ti atoms ("Al_4Ti_2-type") or of two Al and four Ti atoms ("Al_2Ti_4-type"). This coordination seems to be unfavourable for C and O interstitials [22, 24]. For a stoichiometric composition no Ti_6-type octahedral sites exist. Lefebvre et al. [31] considered the case when the Ti concentration of binary TiAl alloys is larger than 50 at.%, which would imply the presences of Ti_6-type sites. They assumed that excess Ti atoms are randomly distributed in the Al sublattice and derived the following equation for the solubility limit $\chi(\gamma)$ (in atomic fraction) of interstitials (in their case O) within the γ-phase [31]:

$$\chi(\gamma) = 2\frac{0.25(2\delta)^2}{1+0.25(2\delta)^2} \qquad \text{(Equation 1).}$$

Here δ is the deviation from stoichiometric composition, i.e. $Ti_{0.5+\delta}Al_{0.5-\delta}$, and has to be inserted as atomic fraction. Using this equation Lefebvre et al. [31] estimated that for a Ti-48Al alloy up to 800 appm of O should be dissolvable within the γ-phase. Measurements performed by Menand et al. [22] for a γ-phase containing 52.5 at.% Ti revealed an O content of 460 $\pm$ 90 appm, a value nearly twice as high as the one obtained for a stoichiometric composition. Similar values of $\approx$ 450 $\pm$ 400 appm O were found within the γ_m-phase of massively transformed Ti-48Al alloys [27, 31], however, it has to be kept in mind that the γ_m-phase has a non-equilibrium composition.

For the case of Nb containing γ-based TiAl alloys it was found experimentally [33, 41-43] and theoretically using various approaches [43-46] that Nb atoms are located exclusively on Ti sites. This implies that Ti antisite defects e.g. Ti atoms on Al sites are formed [43-46]. For the model of Menand and co-workers this means it is even more likely that Ti_6-type sites are formed for Nb-containing γ-based TiAl alloys possessing excess Ti atoms. This in turn should increase the solubility limit of C and/or O within the γ-phase. Using Equation 1 we can estimate for our Ti-45-Al-5Nb-0.5C alloy (if we assume in a first approximation that all Nb atoms contribute to the off-stoichiometric composition, i.e. δ = 0.054) that the maximum solubility limit of C within the γ-phase is $\approx$ 0.6 at.%. Thus, our

obtained value (0.26 at.%) is still below the solubility limit according to the model of Menand and co-workers [27, 31]. In addition it can explain why Nb-doped alloys which contain a higher amount of Al than Ti possess a low solubility limit. For these cases no Ti_6-type cavities are formed (see Table 2).

Experimental results [46] and calculations [45] have shown that Cr and V can substitute both, Ti and Al sites in γ-TiAl. In Al-rich alloys, they can locate at Ti sites while in Al-lean alloys they might substitute Al, whereby for Cr the tendency is higher to occupy Al sites [45, 46]. Taken this into consideration, the number of Ti_6-type octahedral sites and thus the solubility limit of C and O might be lower for alloys containing V, Cr and/or Nb compared to purely Nb doped alloys possessing a similar (low) Al concentration. This can explain the experimental data summarized in Table 2. For example in the work of Gerstl et al. [35] the lower C concentration within the γ-TiAl phase might be related to the presences of Cr additives (besides the fact that the total amount of intentionally added C is lower than for our alloy). In contrast, the reason that Qin et al. [28] observed a relatively low C concentration is attributed to the low amount of C impurities in their alloy.

Following the idea that the formation of Ti_6-type octahedral sites are responsible for a higher solubility limit of C (or O), it should be possible to achieve a similar high solubility simply by using an Ti-rich binary alloy instead doping with Nb. However, the simple model does not consider any energy considerations. It might be energetically favourable that C atoms locate, in addition to the Ti_6-type sites, in e.g. Al_4Nb_2-type cavities, due to the difference in electronic structure between Nb and Ti. How this might affect the solubility can be only predicted by theoretical approaches.

For the sake of completeness we address the question of the C content in the α_2-phase. As Table 1 demonstrates, the average C content in the γ-phase of our material is around 0.25 at.%, which is a factor of two lower than the total C content. Since the volume content of the γ-phase is around 80 vol.% [18], we can estimate that the C content of the α_2-phase should amount to 1.5 at.%. For this estimation we have neglected possible C enrichments at grain boundaries and interfaces which have been reported to exist in some binary TiAl alloys [22,

24] but have not been detected until now for ternary alloys [26, 35]. Nevertheless, it can be speculated that the amount of C in the α_2-phase is much higher than in the γ-phase and possibly larger than > 1 at.%, an assumption which has to be proven by further atom probe measurements. This estimated value is similar to the sum of the O and C content measured by [35] in α_2-lamellae and in the order of the O content found by [21, 22, 24].

The estimated high C content of the α_2-phase in our material can explain the distinct increase in the lattice parameters compared to the C-free case (an increase from 0.46431 nm to 0.46564 nm for the *c*-axis and from 0.57706 nm to 0.57781 nm for the *a*-axis of the hexagonal unit cell, the maximum error for the data is 0.00005) as has been measured by XRD [18]. For the γ-phase, a smaller increase in the lattice constants from 0.40195 nm to 0.40200 nm for the *a*-axis and from 0.40637 nm to 0.40652 nm for the *c*-axis of the tetragonal unit cell (the maximum error for the data is 0.00001) occurred [18] due to the lower amount of C. Similar results had been found by Perdrix et al. [15] for fully lamellar Ti-48Al alloys containing C. Nevertheless, as discussed further below, we can correlate the improvement in strength of our material mainly to a C solid-solution mechanism of the γ-phase, and the strengthening of the α_2-phase is additionally beneficial. That the α_2-phase is harder due to the C in solid-solution has been demonstrated by Perdrix et al. [15].

Strengthening Effect of C in Solid-Solution

As mentioned above, our mechanical tests [18] had shown that the RT tensile yield strength for the C-containing sheet is 270 MPa higher than the C-free Ti-45Al-5Nb-material, although the type of microstructure as well as the volume fraction of the α_2- and γ-phase were similar. The only microstructural difference which we had found was a change in γ-grain size from 10 µm for the C-free sheet to 6 µm for the C-containing material. As discussed in our earlier work, according to a Hall-Petch mechanism this should lead to an increase in yield strength of ~ 90 MPa, which is only one third of the measured value [18]. To estimate whether the detected amount of C in solid-solution within the γ-phase

can account for the further increase in yield strength $\Delta\sigma$, we used the following equation [47]:

$$\Delta\sigma = \frac{1}{\sqrt{3}} m_T \frac{1}{2(1+\nu)} E \eta^{\frac{3}{2}} \sqrt{x} \qquad \text{(Equation 2).}$$

In this equation possible diaelastic contributions are neglected. Here, m_T is the Taylor factor, ν the Poisson number, E the elastic modulus of the alloy, η is related to the change of the lattice constants with the C concentration ($\eta \approx \frac{1}{a}\frac{da}{dx}$) and x the atomic fraction of C. For our alloy $E \approx$ 160 GPa [48], the Taylor factor m_T, = 3.06 and the Poisson number ν = 0.23. η_γ amounts to 0.08 $\pm$ 0.01 and x_γ = 0.00258 $\pm$ 0.00003 for the γ-phase. If we insert these values into Equation 2, we obtain for the increase in yield strength caused by solid-solution strengthening of the γ-phase a value of $\Delta\sigma_\gamma$ = 130 ± 25 MPa. The error is mainly determined by the error of η. The strengthening effect of the α_2-phase due to C can be assessed in a similar way. If we use the estimated value for $x_{\alpha 2}$ of 0.015 and consider that $\eta_{\alpha 2}$ = 0.11 $\pm$ 0.01, we obtain a value of $\Delta\sigma_{\alpha 2}$ = 510 ± 70 MPa. The yield strength of the sample can then be derived from a simplified model, which depends on the volume fraction *f* of the two phases:

$$1/\Delta\sigma \sim f_\gamma / \Delta\sigma_\gamma + f_{\alpha 2} / \Delta\sigma_{\alpha 2} \qquad \text{(Equation 3).}$$

Using equation 3, we obtain for $\Delta\sigma \approx$ 155 MPa. Together with the increase related to the change in grain size of 90 MPa, we obtain a value of $\approx$ 245 MPa, in good agreement to the experimental value of 270 MPa. The difference might be related to equation 2, which is derived for cubic systems, and to the neglect of paraelastic contributions.

The room temperature (tensile) yield strength measured for our samples is much higher than yield strengths values reported in literature for TiAl alloys containing C. For example, Tian and Nemoto [12] reported maximum room temperature 0.2% compressive yield strength values of around 560 MPa for as-

quenched binary Ti-50Al-0.5C alloys, which contained carbon in solid-solution. Their maximum peak strength was 800 MPa which was obtained after thermal aging to form Ti_3AlC Perovskite-precipitates. Similar results were reported by Appel and co-workers [14, 16, 17] for $\sigma_{1.25\%}$ flow stress values. For the homogenized and quenched Ti-48.5Al-0.4C material the value was around 600 MPa at room temperature and it increased to around 870 MPa after age hardening. We attribute the higher strength in our samples, compared to ones observed in these earlier studies, mainly to a higher amount of C which is present in the γ-phase, as a result of the higher Ti:Al ratio and the Nb content, which leads to an increase in the C solubility.

Summary and Conclusions

The chemical composition of the γ-phase of a Ti-rich Ti-45Al-5Nb-0.5C alloy was analysed by atom probe investigations. The results showed that in most areas the C is homogenously distributed, with only a few C rich features present, which are most likely to be dislocations decorated with C. The quantitative analyses revealed that around 0.25 at.% C is dissolved within the γ-phase, a value much higher than those reported in literature. We attribute this to the difference in the alloy chemistry and have been able to explain our results with the help of existing models. The key seems to be the formation of Ti antisite defects, which occur in the alloy due to the addition of Nb. The high C content has a beneficial effect on strength via solid-solution hardening. Taking into account the C solid-solution strengthening and the small change in the grain size, the predicted increase in yield strength is within 10% of the measured value.

Acknowledgements

Fruitful discussion with R. Gerling and G. Dehm are kindly acknowledged. Many thanks to A. Stark for the lattice parameters. The UK facility for atomic scale analysis at Oxford (opal) has been established with funding from the Engineering and Physical Sciences Research Council (EPSRC) under grant number EP/077664/1. Access to opal was funded under the ESTEEM project.

Figure Captions:

Figure 1:

(a) Back-scattered SEM image showing the general microstructure of the primary annealed Ti-45-Al-5Nb-0.5C sheet. The γ-grains appear grey to black, and the α_2-grains white. (b) TEM bright-field image revealing that dislocation are present within γ-twins. Some dislocations are marked with arrows.

Figure 2:

3D-reconstruction of an analyzed volume (60x60x250 nm^3) from the γ-phase showing the homogenously distribution of Ti, Al, Nb, C and Si atoms. The data were acquired in voltage mode using a 3DAP.

Figure 3:

(a) 3D elemental distribution of Ti, Al, Nb, C and Si atoms within the γ-phase of the investigated Ti-45-Al-5Nb-0.5C alloy. Besides two C enriched features, the C is homogenously distributed. (b) Enlarged view of the topmost C rich feature. The data were taken by laser-assisted APT using a LEAP system.

References

[1] Gamma Titanium Aluminides 2003. In: Kim YW, Clemens H, Rosenberger AH, editors. TMS 2003. Warrendale, PA, 2003.

[2] Kestler H, Clemens H. In: Leyens C, Peters M, editors. Titanium and Titanium Alloys. Weinheim, Germany: Wiley-VCH GmbH & Co. KGaA, 2003. p.351.

[3] Structural Aluminides for Elevated Temperature Applications. In: Kim YW, Morris D, Yang R, Leyens C, editors. TMS 2008. Warrendale, PA: in print, 2008.

[4] McAndrew JB, Kessler HD. Trans AIME 1956;206:1348.

[5] Martin PL, Mendiratta MG, Lipsitt HA. Met Trans A 1983;14:2170.

[6] Kim YW. JOM 1989;41:24.

[7] Kim YW, Dimiduk DM. JOM 1991;43:40.

[8] Chen GL, Zhang WJ, Liu CZ, Li SJ. Gamma titanium aluminides. In: Kim YM, Dimiduk DM, Loretto MH, editors. TMS 1999. Warrendale (USA), 1999. p.371.

[9] Appel F, Oehring M, Wagner R. Intermetallics 2000;8:1283.

[10] Zhang WJ, Deevi SC, Chen GL. Intermetallics 2002;10:403.

[11] Kawabata T, Tadano M, Izumi O. Scripta Met 1988;22:1725.

[12] Tian WH, Nemoto M. Intermetallics 1997;5:237.

[13] Chen S, Beaven PA, Wagner R. Scripta Met et Mater 1992;26:1205.

[14] Appel F, Brossmann U, Christoph U, Eggert S, Janschek P, Lorenz U, Mullauer J, Oehring M, Paul JDH. Adv Eng Mat 2000;2:699.

[15] Perdrix F, Trichet MF, Bonnentien JL, Cornet M, Bigot J. Intermetallics 2001;9:807.

[16] Christoph U, Appel F, Wagner R. Static and dynamic strain aging in two-phase gamma-titanium aluminides. In: Koch CC, Liu CT, Stoloff NS, Wanner A, editors. High-Temperature Ordered Intermetallic Alloys Vii, vol. 460. 1997. p.207.

[17] Appel F, Christoph U, Wagner R. Solution and precipitation hardening in carbon-doped two-phase gamma-titanium aluminides. In: Koch CC, Liu CT, Stoloff NS, Wanner A, editors. High-Temperature Ordered Intermetallic Alloys Vii, vol. 460, 1997. p.77.

[18] Gerling R, Schimansky FP, Stark A, Bartels A, Kestler H, Cha L, Scheu C, Clemens H. Intermetallics 2008;16:689.

[19] Miller MK, Cerezo A, Hetherington MG, Smith GDW. Atom Probe Field ion Spectroscopy. Oxford: Clarendon Press, 1996.

[20] Menand A, Chambreland S, Martin C. J de Phys 1986;47:197.

[21] Huguet A, Menand A. Appl Surf Sci 1994;76-77:191.

[22] Menand A, Huguet A, Nérac-Partaix A. Acta Mater 1996;44:4729.

[23] Kim S, Smith GDW. Mater Sci Eng A 1997;239-240:229.

[24] Denquin A, Naka S, Huguet A, Menand A. Scripta Met et Mater 1993;28:1131.

[25] Hono K, Abe E, Kumagai T, Harada H. Scripta Mater 1996;35:495.

[26] Kim S, Smith GDW, Roberts SG, Cerezo A. Mater Sci Eng A 1998;250:77.

[27] Menand A, Zapolsky-Tatarenko H, Nerac-Partaix A. Mater Sci Eng A 1998;250:55.

[28] Qin GW, Smith GDW, Inkson BJ, Dunin-Borkowski R. Intermetallics 2000;8:945.
[29] Wesemann J, Falecki W, Frommeyer G. Phys Stat Sol A 2000;177:319.
[30] Lefebvre W, Loiseau A, Menand A. Ultramicroscopy 2002;92:77.
[31] Lefebvre W, Menand A, Loiseau A, Blavette D. Mater Sci Eng A 2002;327:40.
[32] Gerstl SSA, Seidman DN, Gribb AA, Kelly TF. Adv Mat & Proc 2004;162:31.
[33] Al-Kassab T, Yuan Y, Kluthe C, Boll T, Liu ZG. Surf Interf Anal 2007;39:257.
[34] Masahashi N, Mizuhara Y. Mater Sci Eng A 1997;223:29.
[35] Gerstl SSA, Kim YW, Seidman DN. Interface Sci 2004;12:303.
[36] Vaumousse D, Cerezo A, Warren PJ. Ultramicroscopy 2003;95:215.
[37] Blavette D, Cadel E, Fraczkiewicz A, Menand A. Science 1999;286:2317.
[38] Wilde J, Cerezo A, Smith GDW. Scripta Mater 2000;43:39.
[39] Miller MK. J Mater Sci 2006;41:7808.
[40] Thompson K, Flaitz PL, Ronsheim P, Larson DJ, Kelly TF. Science 2007;317:1370.
[41] Mohandas E, Beaven PA. Scripta Met et Mater 1991;25:2023.
[42] Rossouw CJ, Forwood CT, Gibson MA, Miller PR. Phil Mag A 1996;74:77.
[43] Hao YL, Xu DS, Cui YY, Yang R, Li D. Acta Mater 1999;47:1129.
[44] Wolf W, Podloucky R, Rogl P, Erschbaumer H. Intermetallics 1996;4:201.
[45] Song Y, Yang R, Li D, Hu ZQ, Guo ZX. Intermetallics 2000;8:563.
[46] Hao YL, Yang R, Cui YY, Li D. Intermetallics 2000;8:633.
[47] Gottstein G. Physical Foundations of Material Science. Berlin: Springer, 2004.
[48] Weller M. unpub data 2006.

Table 1:
Chemical composition of the γ-phase in a rolled and primary annealed Ti45Al5Nb0.5C sheet as determined by atom probe analysis. More than 11 Million atoms have been analysed.

Element	Titanium	Aluminium	Niobium
Concentration (at.%)	49.81 ± 0.03	44.21 ± 0.02	5.54 ± 0.01
Element	Carbon	Silicon	Oxygen
Concentration (appm)	2610 ± 10	1650 ± 10	140 ± 4

Table 2

Comparison of the chemical composition of the γ-phase measured by atom probe analysis in various Nb, V- and/or Cr-bearing TiAl alloys containing C and O. Data are taken from [20, 22, 26, 28, 35] and the present work. For the nominal composition ("Alloy") only the main alloying elements are listed. For the data listed with an "*" C was intentionally added.

Element / Alloy	Ti [at.%]	Al [at.%]	Nb [at.%]	Cr and/or V [at.%]	C [appm]	O [appm]	Other [at.%]
Ti-52Al-3Nb [22]	45.2	51.5	3.3	-	130	210	balance
Ti-51Al-5Nb [22]	45.9	48.6	5.5	-	96	265	balance
Ti-48Al-2Cr [26]	48.5	49.5	-	1.9	340	380	balance
Ti-47Al-2Nb-1Cr-1V [28]	49.1	46.4	2.8	0.8/0.8	200	800	balance
Ti-46.5Al-3Nb-1.5Cr [35]	49.4	43.9	3.1	1.8	*1500	800	balance
Ti-45Al-5Nb this work	49.1	45.1	5.4	-	*2580	130	balance

Figure1a

Click here to download high resolution image

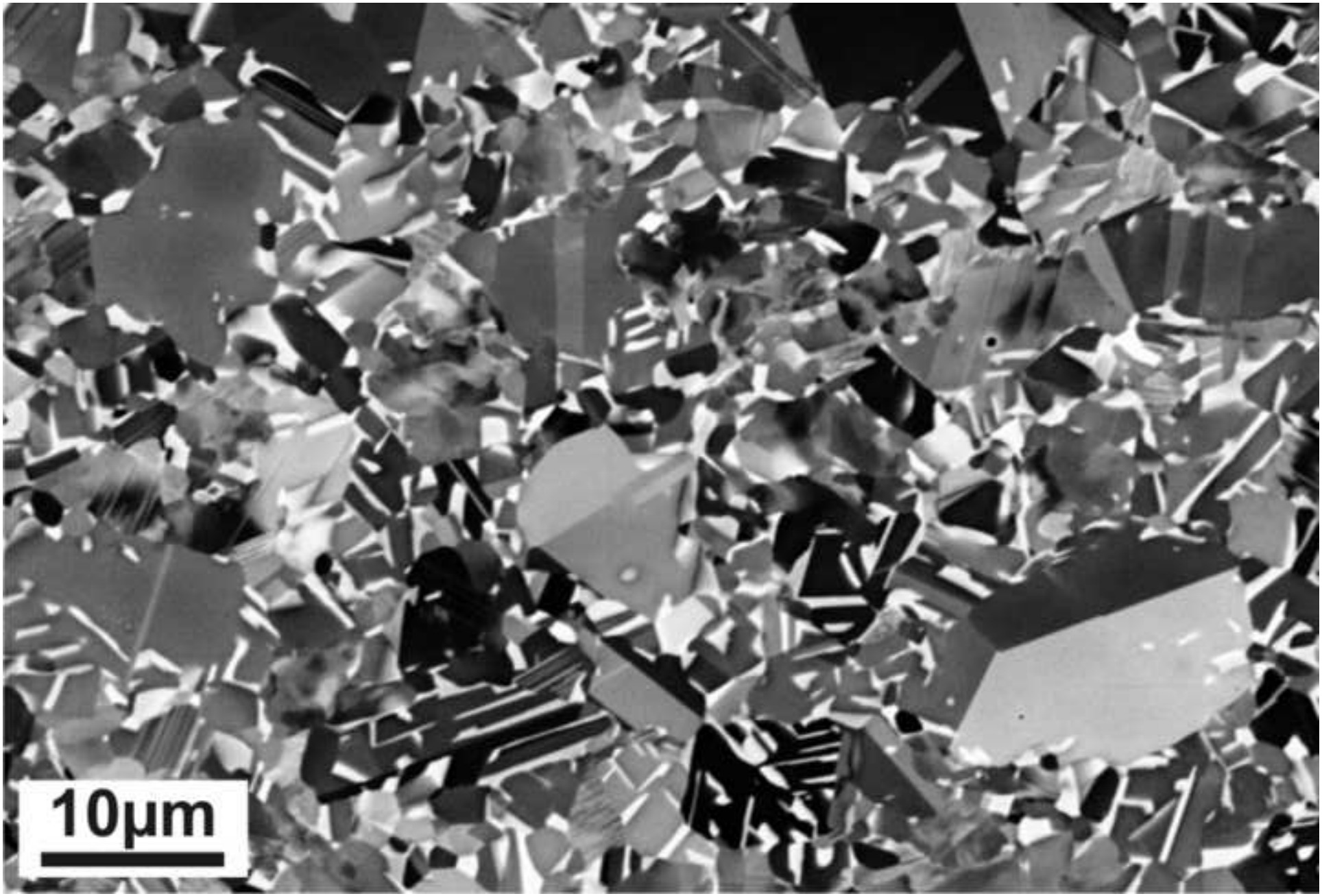

Figure1b

Click here to download high resolution image

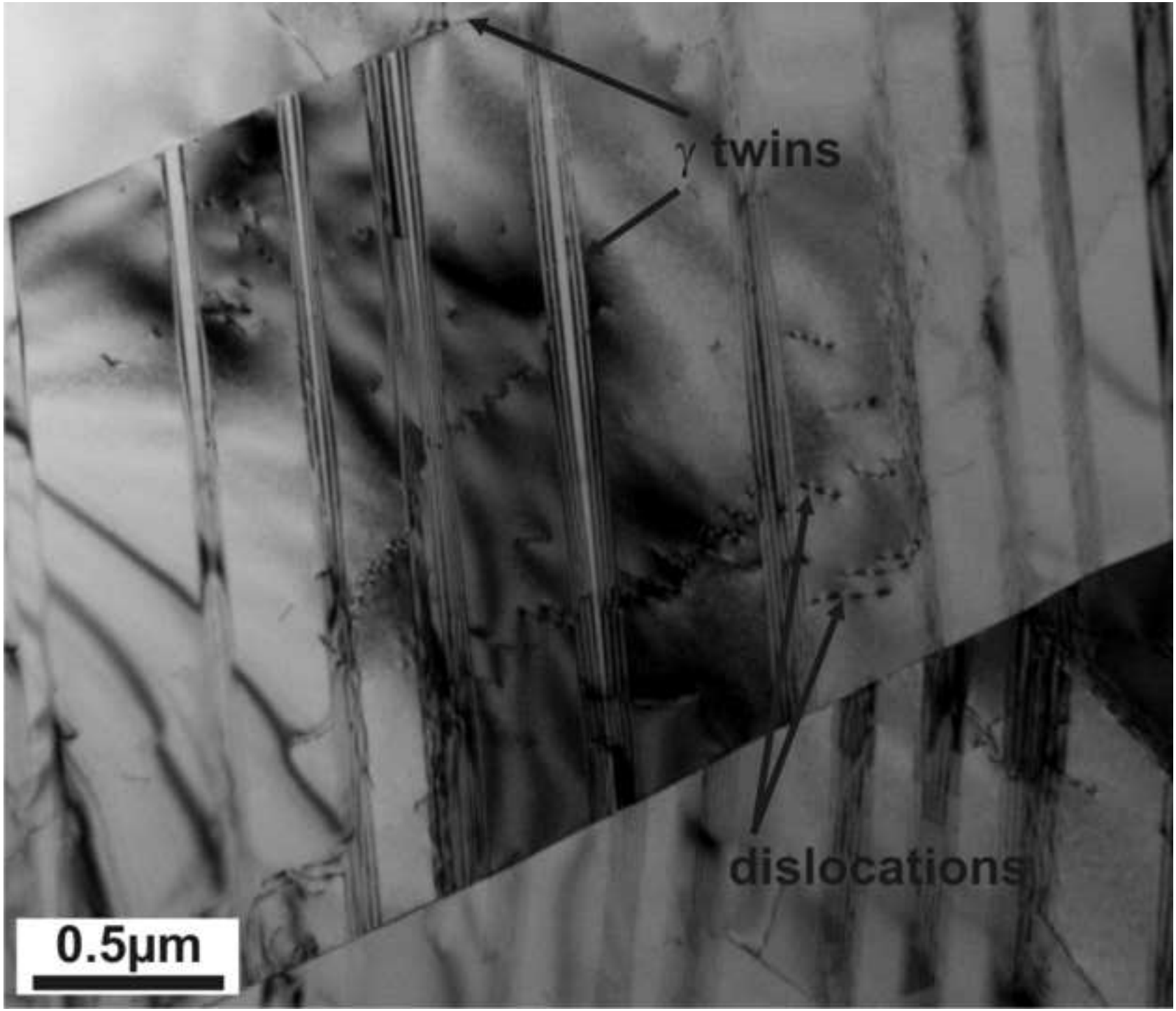

Figure2
Click here to download high resolution image

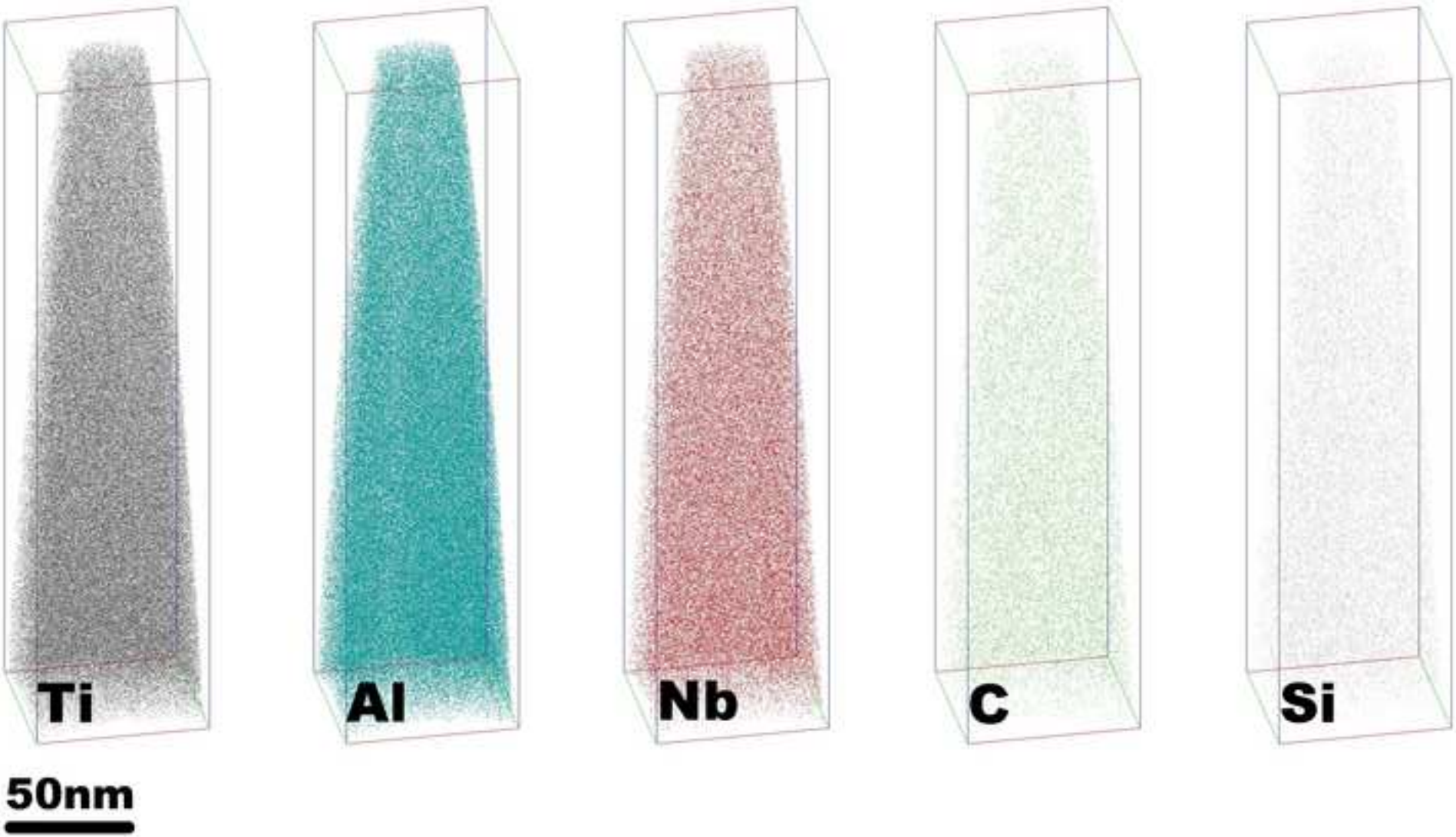

Figure3a

Click here to download high resolution image

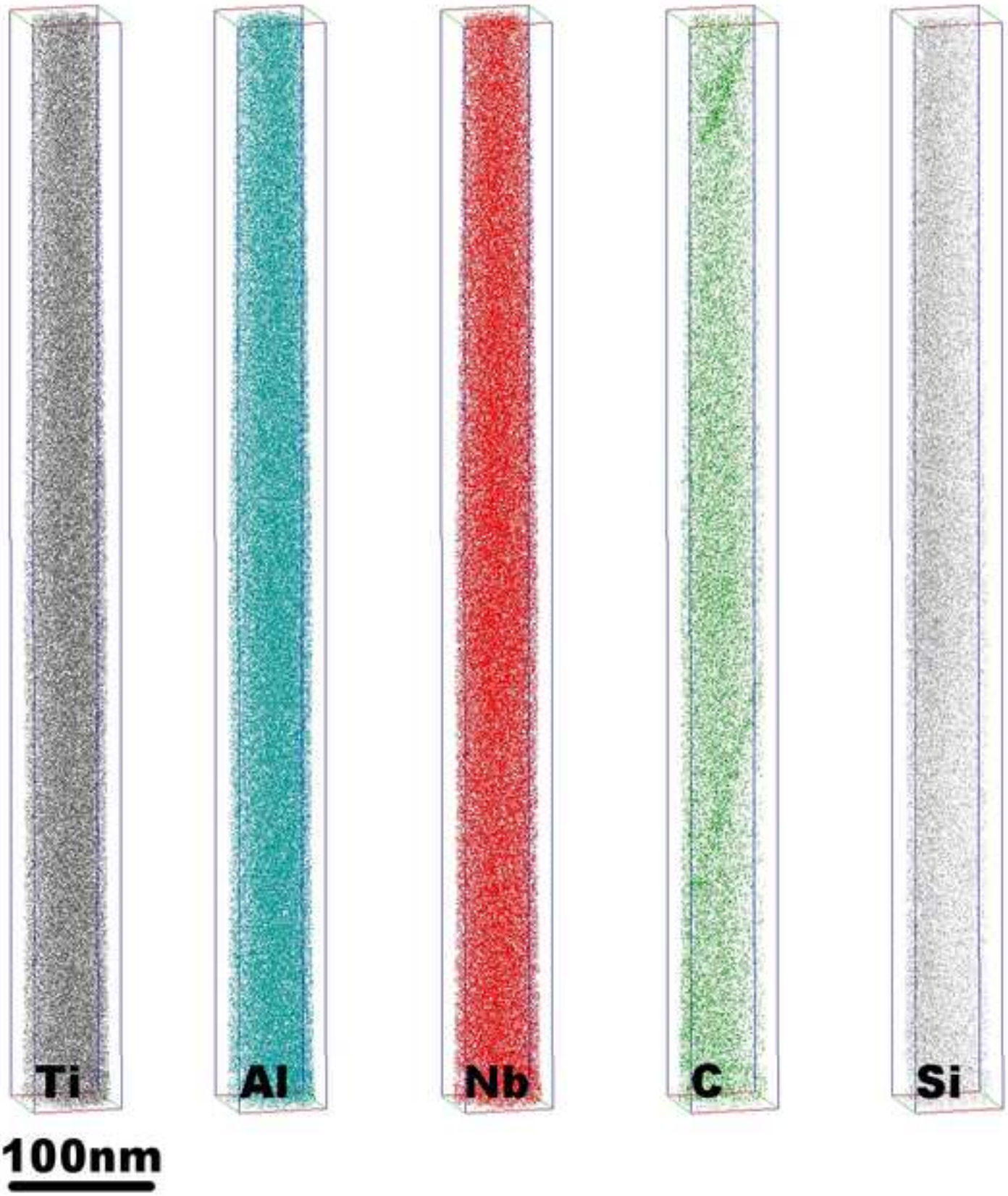

Figure3b

Click here to download high resolution image